Deterioration estimation of paintings by means of combined 3D and hyperspectral data analysis

Luís Granero-Montagud[a], Cristina Portalés[b], Begoña Pastor-Carbonell[a], Emilio Ribes-Gómez[a], Antonio Gutiérrez-Lucas[a], Vivi Tornari[c], Vassilis Papadakis[c], Roger M. Groves[d], Beril Sirmacek[d], Alessandra Bonazza[e], Izabela Ozga[e], Jan Vermeiren[f], Koen van der Zanden[f], Matthias Föster[g], Petra Aswendt[g],Albert Borreman[h], Jon D. Ward[i],António Cardoso[j], Luís Aguiar[j], Filipa Alves[j], Polonca Ropret[k], José María Luzón-Nogué[l], Christian Dietz[l]

[a]AIDO, Optics, Color and Image Institute of Valencia,C/ Nicolás Copérnico, 7 - 11, 46980 Paterna, Spain; [b]IRTIC (Instituto de Robótica y Tecnologías de la Información y las Comunicaciones),Universidad de Valencia,C/ Catedrático José Beltrán 2, 46980, Paterna,Spain, [c]FORTH, Foundation for Research and Technology Hellas,P.O. Box 1527,GR-711 10 Heraklion, Greece; [d]Optical Non-Destructive Testing Laboratory,Faculty of Aerospace Engineering, Delft University of Technology, Postbus 5058, 2600 GB Delft, The Netherlands; [e]CNR-ISAC, Consiglio Nazionale delle Ricerche,Via Gobetti 101, 40129 Bologna, Italy; [f]XENICS NV Ambachtenlaan 44, BE-3001 Leuven, Belgium; [g]VIALUX GmbH Am Erlenwald 10, 09128 Chemnitz, Germany;[h]AVANTES BV Oude Apeldoornseweg 28, 7333 NS Apeldoorn, The Nederlands; [i]Gooch & Housego Ltd Dowlish Ford, Ilminster, Somerset, TA19 0PF, United Kingdom; [j]SIGNINUM - Gestão de Património Cultural Rua Sete, n. 85, Paredes, 4845-024 Rio Caldo, Portugal; [k]IPCHS, Institute for the Protection of Cultural Heritage of Slovenia Metelkova 6, 1000 Ljubljana, Slovenia; [l]RABASF, Real Academia de Bellas Artes de San Fernando Alcalá , 13, 28014 Madrid, Spain

ABSTRACT

Deterioration of artwork, in particular paintings, can be produced by environmental factors such as temperature fluctuations, relative humidity variations, ultraviolet radiation and biological factors among others. The effects of these parameters produce changes in both the painting structure and chemical composition. While well established analytical methodologies, such as those based in Raman Spectroscopy and FTIR Spectroscopy require the extraction of a sample for its inspection, other approaches such as hyperspectral imaging and 3D scanning present advantages for in-situ, non-invasive analysis of artwork. In this paper we introduce a novel system and the related methodology to acquire process, generate and analyze 4D data of paintings. Our system is based on non-contact techniques and is used to develop analytical tools which extract rich 3D and hyperspectral maps of the objects, which are processed to obtain accurate quantitative estimations of the deterioration and degradation present in the piece of art. In particular, the construction of 4D data allows the identification of risk maps on the painting representation, which can allow the curators and restorers in the task of painting state evaluation and prioritize intervention actions.

Keywords: artwork deterioration, 3D scanning, hyperspectral imaging.

1. INTRODUCTION

According to the EGMUS - European Group on Museum Statistics there are, approximately, 21,000 institutions across Europe that exhibit art in permanent or temporary collections and have a key role in the sustainability of cultural heritage by joining the importance of culture dissemination and tourism as an exploitation market, in line with the UNESCO's Word Heritage and Sustainable Tourism Programme (Action Plan 2013-2015). For these organizations, cultural heritage monitoring comprehends an essential routine and requires employing a range of equipment, technologies and protocols to achieve the most detailed information about how the passage of time and the environment contribute to deterioration, change or weakening of the artworks. Moreover, the accuracy of monitoring techniques nowadays becomes more important as the durability of an artwork depends on the materials of which it is composed and detecting molecular

changes, due to complex processes such as ageing and environmental climate effects, and is indispensable for the purpose of a proper restoration and conservation. To achieve this, restorers and collection owners need to address four aspects:

- Handling restrictions: the artwork transport could mean important risks due to unknown data about the initial state and stability.
- Steps in the characterization: the complete measurement of deterioration parameters requires the application of some different techniques separately with a direct consequence in time consumption and wider data analysis.
- Bad cost-benefit ratio: the use and maintenance of these equipments represent a high expenditure/investment respecting the data achieved in the time spent, and that produces a poor exploitation of these techniques and a gap in the artwork study.
- Imprecision due to extrapolation: the study of whole artworks is difficult to perform since the current routine takes random or limited samples.

The main objective of the presented work is to develop a prototype instrument for monitoring the deterioration of artworks. This will be achieved by using 3D data with the addition of hyperspectral imaging. Being optical, the technique is non-invasive and therefore non-destructive. We propose a new combination of 3D scanning techniques and hyperspectral imaging that could widely reduce and increase inspection accuracy, while reducing time and costs in the characterization of art assets, speeding up the analysis procedures and minimizing the impact of manipulating and transportation on the artwork. To successfully develop such prototype, a series of technical and project operational considerations have been stated, as follows:

- 3D digitization. Our system includes 3D imaging capabilities by means of a digital light project (DLP) which projects light-on-light-off patterns on the objet for 3D digital surface reconstruction.
- Hyperspectral imaging in the visible range. The system provides sensitivity in the visible range (400nm to 720nm), acquiring hyperspectral bands with 20 nm bandwidth.
- Types of evaluated cultural assets. We have focused our study in analyzing paintings on canvas and wooden panels within the Baroque period. The system produces 4D models (3D+hyperspectral) of each of the assets analyzed, for deterioration information extraction.
- Deterioration evaluation due to environmental conditions. The effects of temperature, relative humidity, ultraviolet radiation and pollutants deposition such as carbon, calcium carbonate and dust are considered.

The main results achieved in this contribution are in the following areas: Digitization and characterization of different types of physical and chemical damages; A method for generating 4D maps of the painting by means of combined hyperspectral and 3D data recording; morphological and spectral feature extraction from the 4D data; development of training algorithms and a validation model for physical and chemical damage detection and quantification.

The paper is organized in six sections. In section 2 we review the state of the art in 3D scanning and analytical techniques focused in art pieces. In section 3 the developed inspection system is introduced. Section 4 explains the followed overall methodology to acquire process, generate and analyze 4D data. In section 5 some of the obtained results so far are depicted. Finally, section 6 is dedicated to the conclusions and further work.

2. 3D SCANNING AND ANALYTICAL TECHNIQUES

Digital recording of cultural heritage is a multidimensional process. It depends highly on the nature of the subject of recording as well as the purpose of its recording. The whole process involves the three-dimensional digitization, color recording, digital data processing and storage, archival and management, representation and reproduction. Optical instrumentation permits the acquisition of complex virtual models from the original artwork with high accuracy. These models allow the study of the structure without a direct handling on the artwork, avoiding damages due to the process.

The construction of 3D surface models of the objects for detailed 3D measurements is a field of ongoing research for some decades. For 3D shape measurement of the objects, commonly used methods can be listed as applying stereo vision

techniques to the images which are acquired from multiple cameras, using one or multiple line laser strips, and using coded light patterns (structured light) for generation of the 3D image data [1, 2]. One technique to mention is fringe projection, which uses a plane of projected light that is viewed by a camera positioned at an angle, such that the camera can view the fringe as it illuminates surfaces over some predetermined range. With this technique is possible to record full-field height measurements of an unknown object surface in the time it takes for a CCD camera to capture an image. The objects typically measured are size, surface texture and shape of the artwork, for whole and partial scans for reverse engineering of art restoration and for reproduction of artworks.

For organizing the obtained point cloud and for generating the surface model, before applying meshing techniques, a point cloud filtering is necessary in order to remove the noisy, mis-measured points from the point cloud which can lead to more pure 3D surface generations. For filtering point clouds, one of the most frequently used methods is filtering the point cloud with a statistical outlier removal filter [3]. This filter works using the distribution of point to neighbor distances in the point cloud. By assuming that distribution as a Gaussian function, all points whose distances to the mean of the Gaussian function are greater than a threshold value can be removed from the dataset. In our study, we would like to benefit from a statistical outlier removal filter design including more intelligent computer vision methods. Therefore, before smoothing the point cloud, in order to not to lose sharpness in damaged areas, we would like to extract some 3D features which can indicate important regions. With a similar idea, some of the researchers aimed to detect the edge and other 3D geometrical features directly from the point cloud [4].

In the related literature many researchers have focused on automatic 3D feature extraction from point clouds. In reference [5], without mesh generation and surface reconstruction, they computed distances to the local neighbor points in order to detect points which have high distances to the neighborhood. Detected points are used to extract more 3D geometric features for detecting sharp shapes on the 3D surfaces. In reference [6], researchers applied line and curve detection by grouping the surface normal from point clouds. They use extracted line and curvatures for feature-preserving mesh construction directly from noisy point clouds. In another study, researchers applied a point classification by checking the surface normal of the neighbors.

3. DESCRIPTION OF THE HARDWARE IMPLEMENTATION

The system here described is designed to acquire 3D data and multiband images in the visible range. It consists of a Digital Light Projector (DLP), a monochromatic camera and a filtering device. The camera has a CMOS sensor with 5MP resolution, 8bit depth and is sensitive in the wavelength range from 390 nm to 1100 nm. The filter is a Liquid Crystal Tunable Filter (LCTF) providing transmission in the wavelength range from 400 nm to 720 nm, having a bandwidth of 20 nm, leading to a total of 16 spectral bands. To generate these bands, it makes use of Gaussian-shaped filtering windows. The DLP unit is an application dedicated device, and its design and construction has been carried out in the field of the presented project. It has a spatial mirror resolution of 1920x1200 and a LED source providing transmission in the range from 250 nm to 750 nm. It also includes a cooling device. Additionally, some optics are introduced between the different components. All the components are attached to a rigid platform which has been designed to be light and portable. These devices are controlled by dedicated software that runs under C++, though the GUI has been designed with the LabView software package. The spatial arrangement of the devices and optics is illustrated in Figure 1.

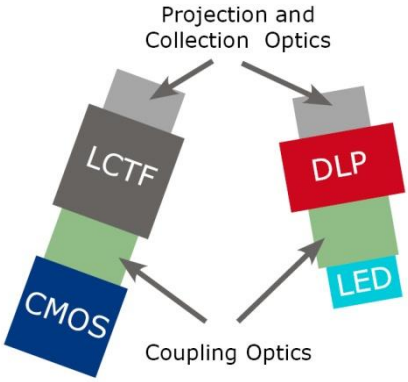

Figure 1. Spatial arrangement of the optical devices.

4. METHODOLOGY

The methodology proposed in this work consists of two defined parts. Firstly, the production of 3D-HS (Hyper Spectral) point clouds is made from data obtained in the visible spectrum with spectral resolution of 20 nm, given by Gaussian-shaped filtering windows. Secondly, processing algorithms are developed for the combined 3D-HS data maps for classification and quantification of deterioration from both structural and a chemical points of view. The generation of the tridimensional point clouds is carried out by means of structured light patterns projected over the painting and recorded at different spectral bands, from 400nm to 720nm. Finally, band fusion techniques are used to generate a single-band, gray-scale image collection of the 2D fringe projection, from which the depth information can be derived. A reconstruction approach based on Fourier transformation and phase shifting has been implemented to generate the 3D point cloud. The analysis of the resulting data sets is processed by means of morphological algorithms which can identify points of structural modification of the due to support, ground and paint and varnish damage. Using supervised linear and nonlinear classifiers, the surface of the painting may be inspected to identify discontinuities and alterations in the pigment and binder application, giving an indication of loss or change in material. Deterioration quantification is given for the following conditions:

- Physical deterioration
- Support damage (crease, dent, tear, bulges, cuts, buckling)
- Ground damage (blisters, aging cracks, cleavage)
- Paint damage (abrasion, alligatoring, crackle, drying cracks, loose, paint, lacunas)
- Varnish physical damage (particle deposition form combustion smoke, craquelure, superficial grime)
- Chemical deterioration
- Pigment alterations (due to light radiation, due to chemical interaction with other elements, due to heat damage)
- Varnish alterations (oxidation, blooming, heat damage)

In Figure 2 a schematic is depicted that shows the overall strategy, which is explained in the following sub-sections point by point. It has to be noted that as this is an ongoing project, some of the here described steps have not been fully implemented and/or tested, though the given strategy is clear and will lead to the fulfillment of our requirements.

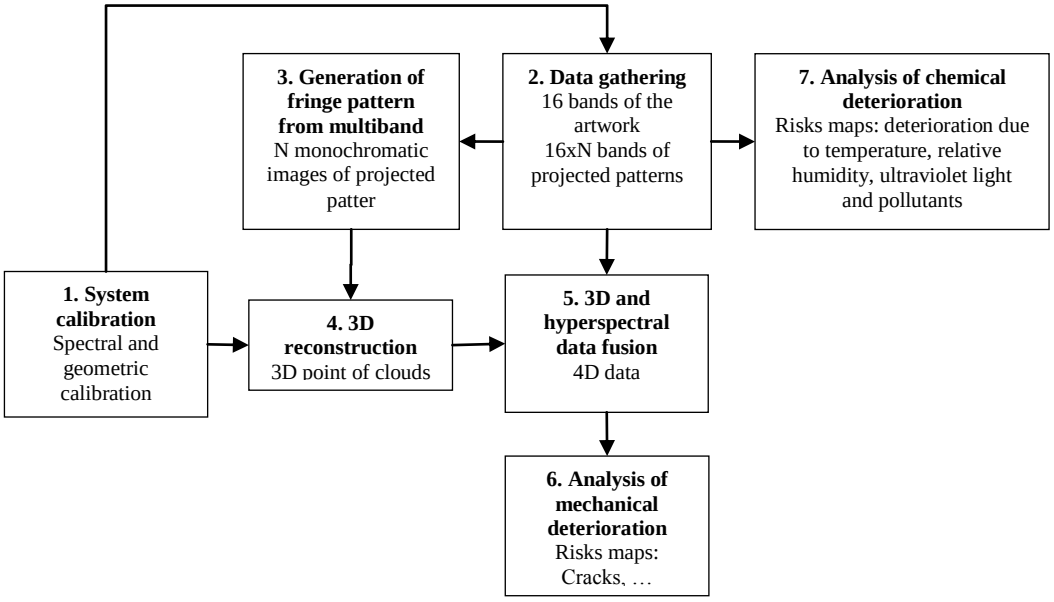

Figure 2. Methodology flow chart.

4.1 System calibration

We have considered two kind of calibration: spectral and geometric calibration. The former is needed in order to equalize the acquired hyperspectral images, where the last will be used in order to make the phase to height conversion in the gathered 3D model.

Regarding to the spectral calibration, the strategy implemented to compensate spectral bands from the inhomogeneous in light consists on acquiring an image of a white reference, and then white balance compensation is applied to the new acquired images.

In the case of geometric calibration we have implemented a method to obtain the interior and exterior parameters of both the hyperspectral camera and the DLP. To that purpose, we have considered the DLP as the equivalent of a camera, i.e. it is considered as a pinhole camera and the intrinsic parameters are equivalent. First the camera is calibrated, and then the projector. To achieve the intrinsic parameters we have implemented a method that is based in finding multiple 2D/3D correspondences of a planar object viewed from different angles. This object is a chessboard, so the 2D points of each square can be automatically found. The 3D coordinates of all points are also known, as we measure the square size of the chessboard (all points have Z=0). In this process, we obtain the focal lengths in both x and y direction, the x and y offsets of the principal point and five distortion coefficients. The algorithm is based on Zhang's method described in [7] to solve the focal lengths and offsets, and the distortion parameters are computed following the method described in Brown [8]. The DLP is calibrated in the same way than the camera. Nevertheless, as the DLP is not able to "see", the projected chessboard, we use the images acquired by the camera to establish 2D/3D correspondences of the projector. Once the interior calibration is known, the chessboard is placed on a single position and two images are acquired by the camera, one image with the physical chessboard, and the other one with a projected chessboard, that is used for the camera to "see" instead of the projector. In this way 2D/3D correspondences are acquired and applying spatial resection the external orientation parameters of both camera and DLP are computed. Once the geometric calibration has been determined, a depth-to-height model can be obtained by applying the procedure introduced in [9] in order to further reconstruct 3D objects (see section 4.4).

4.2 Data gathering

The system collects a set of images of each inspected artwork. On one hand it captures the 16 bands by illuminating the artwork with white light. These bands will be used to construct spectral curves for the chemical deterioration analysis (see section 4.7). On the other hand it captures another 16 bands by projecting a pattern of fringes, which is further shifted. These images will be used for the 3D reconstruction (see sections 4.3 and 4.4). Considering that the pattern of fringes is shifted N times, the system will acquire a total of 16(1+N) images per inspection (16 with white light + 16xN with projected and shifted patterns).

4.3 Generation of fringe pattern from multiband

In order to obtain 3D models (explained in next section), an image of a projected fringe pattern should be gathered. As the system provides 16 different bands, they have to be properly combined in order to obtain a single image that contains all the required spectral information and where the fringe patterns appear enough contrasted to further apply the 3D reconstruction. A sample on the strategy used to generate a pattern from multiband information is shown in Figure 3. In first place, the different spectral bands are captured by the camera, each one corresponding to different filtered wavelengths with Gaussian-shaped filtering windows. For each of the multidimensional pixels, the spectral response as acquired by the camera can be represented as indicated by the red line of the middle top graph in Figure 3. In this graph, the black line represents the continuous spectral response, where the red line is the discrete solution recovered by the camera, with the same dimensions as the number of bands. The blue lines represent the Gaussian filters applied by the filtering device in normalized values. The discrete values of the red line are multiplied by the camera quantum efficiency at those positions. Finally, each of the pixels at the composed image is obtained by adding all the multiplications, and then dividing by the total number of bands.

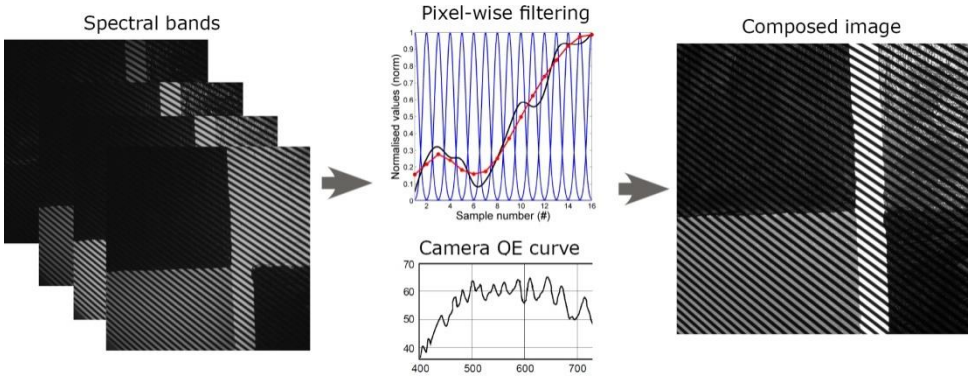

Figure 3. Composition of a monochromatic image from a set of bands, where: left images are some of the sampled bands; the graph at the middle top corresponds to a sample of an spectral curve at one multidimensional pixel (red), its theoretical continuous value (black) and the Gaussian filters (blue); the graph at the middle down corresponds to the camera quantum efficiency curve, showing the efficiency from 400 to 720 nm; the right image corresponds to the monochromatic composed image.

4.4 3D reconstruction

To reconstruct the height of the inspected artworks we have implemented a method based on structured light. Coded structured light systems are based on the projection of one pattern or a sequence of patterns onto the object's surface. Due to the differences in the object height, the projected pattern appears distorted when viewed obliquely. Therefore, the fringe pattern is modulated according to the object's 3D height and the angle formed between the illumination and the viewing axes. The height profile of the object appears encoded as a function of the spatial phase of the fringe pattern, i.e. the object's height modulates the intensity distribution of the fringe pattern as expressed in the next equation [10]:

$$g(x,y) = a(x,y) + b(x,y)\cos(2\pi f_0 x + \varphi(x,y)) \quad (1)$$

Where *a(x,y)* represents the background illumination, *b(x,y)* is the amplitude modulation of fringes, f_0 is the spatial carrier frequency, and $\varphi(x,y)$ is the phase modulation of fringes.

Pattern projection techniques differ in the way in which every point in the pattern is coded and decoded. Our implementation is based on a combination of the Takeda method [10, 11] and phase shifting, in a similar way as described in [12]. The method introduced by Takeda is based on applying a Fast Fourier Transformation (FFT) and can be used to reconstruct 3D objects with a single image that contains a projected fringe pattern (Figure 4). Nevertheless, by projecting a set of images with a phase shifting, the unwanted background variation $a(x,y)$ that represents the zero order can be automatically filtered. In the same process, other superior orders can be filtered, thus obtaining an image with the first order. Afterwards, the first order is selected and translated by f_0 on the frequency axis towards the origin. The demodulation of fringe patters results in a so-called wrapped phase ψ instead of the required phase φ. Therefore, a phase unwrapping is required to recover φ. Nevertheless, a direction warping can appear due to the perspective distortion introduced by the projector-camera pair; for instance, if the central projection axis of the projector is not orthogonal to the registered object, fringes that are closer to the projector will appear narrower than those located further away; in the same way, the location of the camera can introduce perspective distortion. In order to correct this effect, a reference plane with fringe patterns can be processed and reconstructed in the same way, and then the depth variations departing from the condition of coplanarity can be subtracted to the unwrapped phase of the object. Finally, the computed phase is extracted and related to actual object height by use of some sort of phase-height relationship that has been previously determined during system calibration.

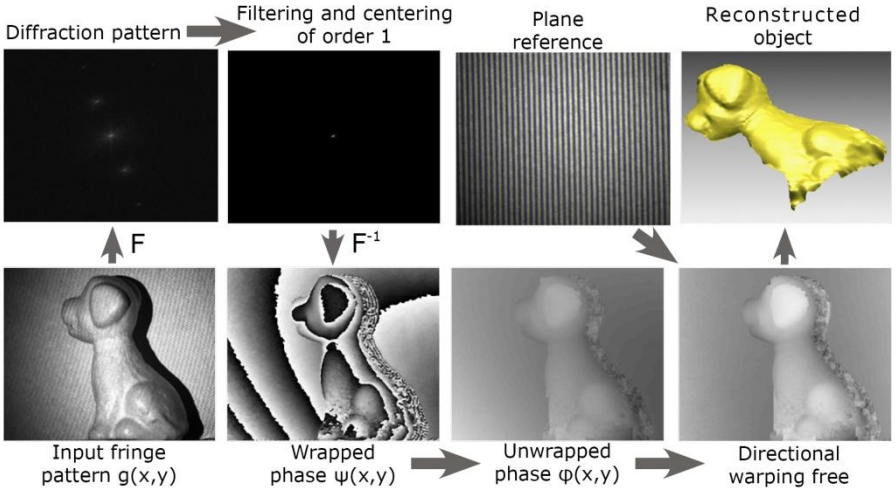

Figure 4. Steps followed to reconstruct an object from fringe projections with FFT.

4.5 3D and hyperspectral data fusion

Data fusion is important for our project for several reasons. First of all, when required, one of the selected hyperspectral bands (or a combination of some of them) should cover 3D surface like a texture. Second, hyperspectral image classification results, which are obtained by using hyperspectral information, should be mapped on 3D surface easily. And a third very important reason is that we should be able to compare the 3D surface or hyperspectral data which are acquired in different times. The geometrical relationship of 3D and hyperspectral data is directly determined, as our system is in fact a 3D camera where each of the image pixels correspond to one height value. Both spatial and spectral information are stored in a single ascii file, constituting in this way what we refer as 4D data.

On the other hand, when comparing artworks obtained at different periods of times, they need to be spatially aligned, a process referred as co-registration. There exist different techniques to perform co-registration, where some of them are based on images and other on 3D models. In co-registration based on images, matching is usually achieved by locating a set of feature points in two images and finding the 2D correspondences between them. Some well-known feature detection algorithms are the Scale Invariant Feature Transform (SIFT), by David Lowe [13], and the Speeded Up Robust Features (SURF), first presented in [14]. As a final step, the perspective matrix that better aligns both set of points is calculated and applied to one of the images, being thus both images co-registered. In co-registration based on 3D models, the Iterative Closest Point (ICP) algorithm could be used. ICP minimizes the difference between two clouds of points, and it is commonly used for registration of rigid objects. For instance, it is often used to reconstruct 2D or 3D surfaces

from different scans, to localize robots and achieve optimal path planning, to co-register bone models, etc. In our case we will use a combination of these techniques, as both 3D and imaging information is available.

4.6 Analysis of mechanical deterioration

The starting point to generate the surface from the point clouds is the moving least-squares (MLS) technique [15]. One of the advantages of this approach is its intrinsic capability to handle noise in the input data and to be able to generate a clean (filtered) surface. MLS is based on a local surface fitting, and it is naturally framed as a statistical approach to surface reconstruction. Furthermore, the MLS technique makes it easy to compute a very accurate calculation of the surface normals of the points on the generated surface.

Surface normals are used to identify deformations in the surface. To estimate the surface normal, the algorithm uses the eigenvector analysis based method which was introduced by Rusu [16]. After calculating the surface normal for each point, differences of the normals within a given radius is calculated. The radius defines the geometrical scale of the regions that over which shape imperfections are investigated, allowing their segmentation from the flat (perfect) surface. In our current implementation, two different radius parameters, r_s (small radius) and r_l (large radius), are chosen as 100 and 2500 points respectively. In this way, small scale and large scale surface imperfections can be displayed. We expect that later versions of our interface will automatically recommend values of r_s and r_l, and allow the user to change these values if necessary. To process the point cloud, the open source Point Cloud Library (PCL) and OpenCV libraries are used.

4.7 Analysis of chemical deterioration

Using supervised linear and nonlinear classifiers, we aim at identifying four types of chemical deterioration, which are deterioration due to temperature, relative humidity, ultraviolet light and pollutants. A dedicated spectral database was gathered in order to train the classifiers. To that purpose four physical probes were prepared that contained a set of pigments which were afterwards deteriorated by the aforementioned agents: one probe was deteriorated in a chamber with ultraviolet radiation; a second probe was deteriorated in a chamber with humidity and temperature; a third probe was deteriorated on the outside by the deposition of pollutants; and the last probe remained unaltered to serve as reference (non-deteriorated pigments). Each probe consisted of 40 different pigment mixtures. These pigments were sampled by our system. Each voxel of the hyperspectral cube can be seen as a spectral curve that is characteristic of each pigment, i.e. the spectral signature of the pigment, forming all together a spectral database of deteriorated and non-deteriorated pigments. Afterwards, these curves were grouped into classes, resulting in a total of 56 classes (if two pigments have similar spectral curves, they belong to a single class). Once the database was created, we proceeded to classify new pigments in order to determine if they have suffered any of the four considered deteriorations.

The implemented classification methodology follows a similar procedure as described in [17], which uses in a first step the Principal Component Analysis (PCA) algorithm in order to reduce data dimensionality. Nevertheless, instead of using a fuzzy rule-based identification system, we have implemented a set of different classification strategies based on supervised methods in order to test their performance. We have implemented a set of six different classifiers based on Euclidean and Mahalanobis distances; additionally we have also implemented Support Vector Machines (SVM) with three different kernels (linear, polynomial and RBS). The idea is to select that classifier that better works in determining pigment deterioration based on experimental results. Our first trials show that all classifiers are above the 80% of success, and some above the 90% with the consideration of 56 classes.

5. RESULTS

5.1 3D acquisition

In this section we show an example of the 3D acquisition process of an artwork piece by following the procedure indicated in section 4.4. In this case, the projected fringe pattern has a period of 4 pixels, and thus to apply the phase shift procedure a total of 4 fringe images are projected. In Figure 5(a) the phase of the image obtained after applying phase shift procedure is depicted, where a detail of a small region is also shown. As it can be observed, the fringes are slightly

distorted due to height differences at the artwork. Figure 5(b) shows the module of the image obtained after applying phase shift. Figure 5(c) shows the module of the Fourier transformation where the first order is depicted. As it can be observed that while the zero order is completely filtered, some higher orders are still present due to some unwanted effects in the acquired image which need to be further considered. Nevertheless these higher orders appear attenuated and the first order can be easily located. After selecting order 1 and translating it towards the origin, the demodulation of the fringe pattern results in the wrapped phase, which is depicted in Figure 5(d). The directional warping that appears due to the perspective is indicated. In Figure 5(e) the desired unwrapped phase is shown. Finally, after applying directional warping correction the depth image is obtained. The result is given in Figure 5(f), where the level of detail is such that brush-strokes can be observed.

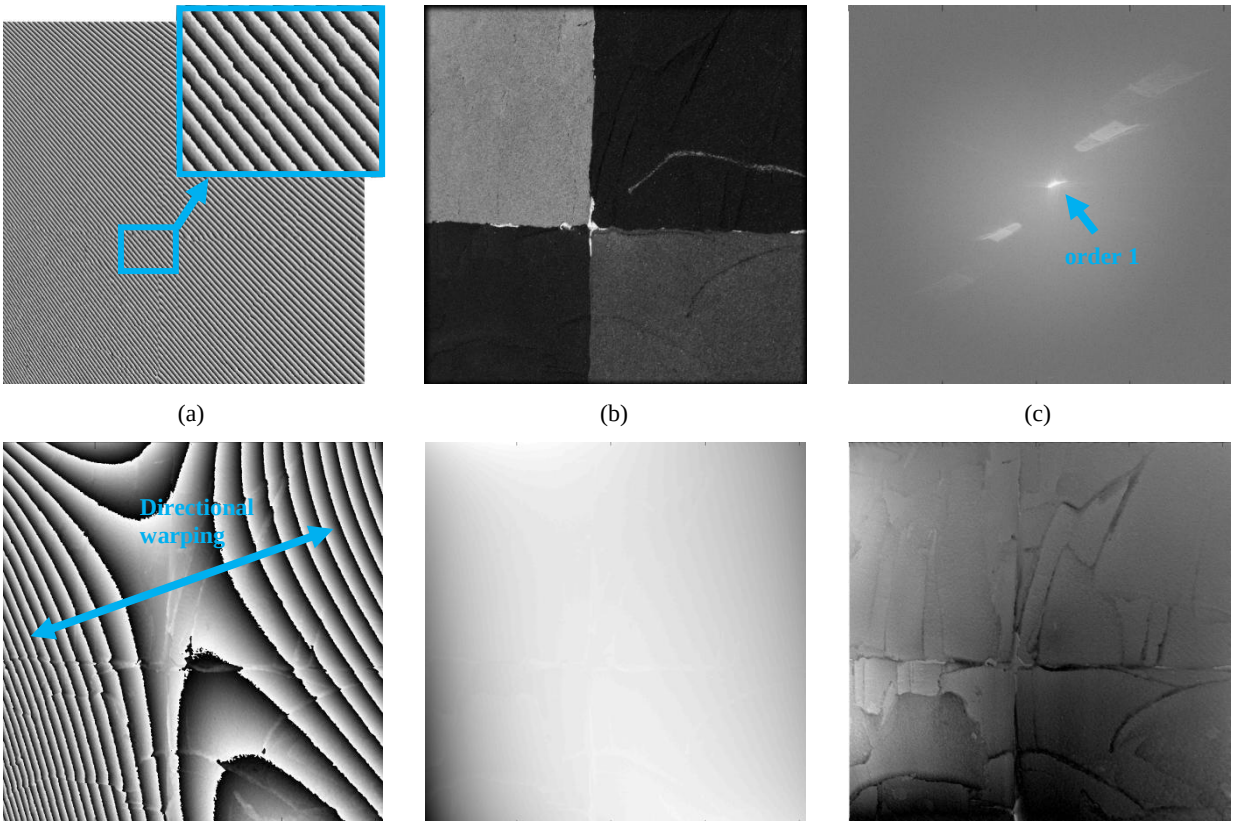

Figure 5. Different images acquired with the 3D reconstruction of an artwork piece by applying FFT and phase shifting, where: (a) phase of the image obtained by applying phase shifting; (b) module of the image obtained by applying phase shifting; (c) module of Fourier transformation, where of order 1 is depicted; (d) wrapped phase; (e) unwrapped phase; (f) depth image after applying directional warping correction.

5.2 Analysis of mechanical deterioration

As an example of analysis of mechanical deterioration, an artwork of the Baroque period has been registered, which belongs to artwork collection of the Real Academia de Bellas Artes de San Fernando (Madrid, Spain). Spectral information is registered and mapped on the point cloud as it is presented in Figure 6(a). This surface mesh shows surface deformations as shown in Figure 6(b).

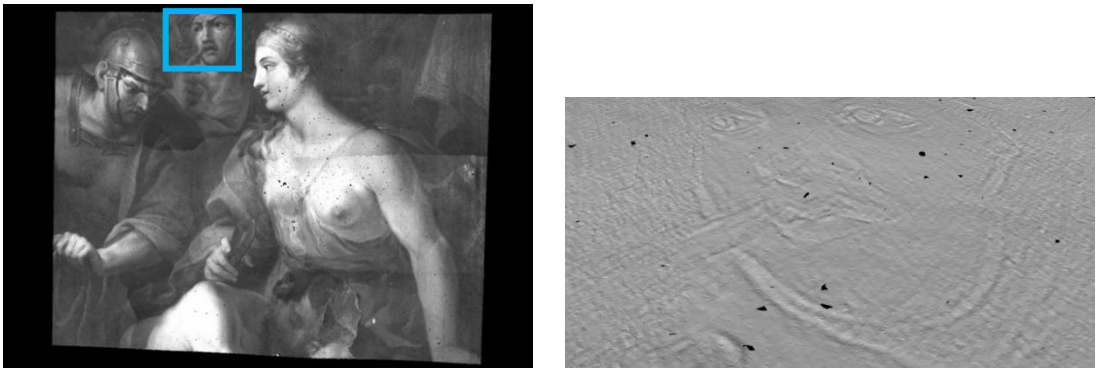

(a) (b)

Figure 6. (a) Spectral values mapped onto the 3D point cloud; (b) T view of the 3D mesh surface for the painting, where the depicted area (tilted) corresponds to the highlighted square of left image.

Figure 7 shows the results from applying the surface normal and deterioration analysis. For the generated 3D surface normal vectors are computed for each point location. The normal vectors are illustrated on 3D mesh surface model in Figure 7(a). After calculating the normal vectors, differences of normals in different scales are computed to understand abnormalities on the surface. For a flat surface, differences of normals give a zero value. However if the surface is not flat, differences of normals in the focus area (depending on selected scale) give a non-zero value. Those non-zero value regions are labeled as deterioration areas on the surface.

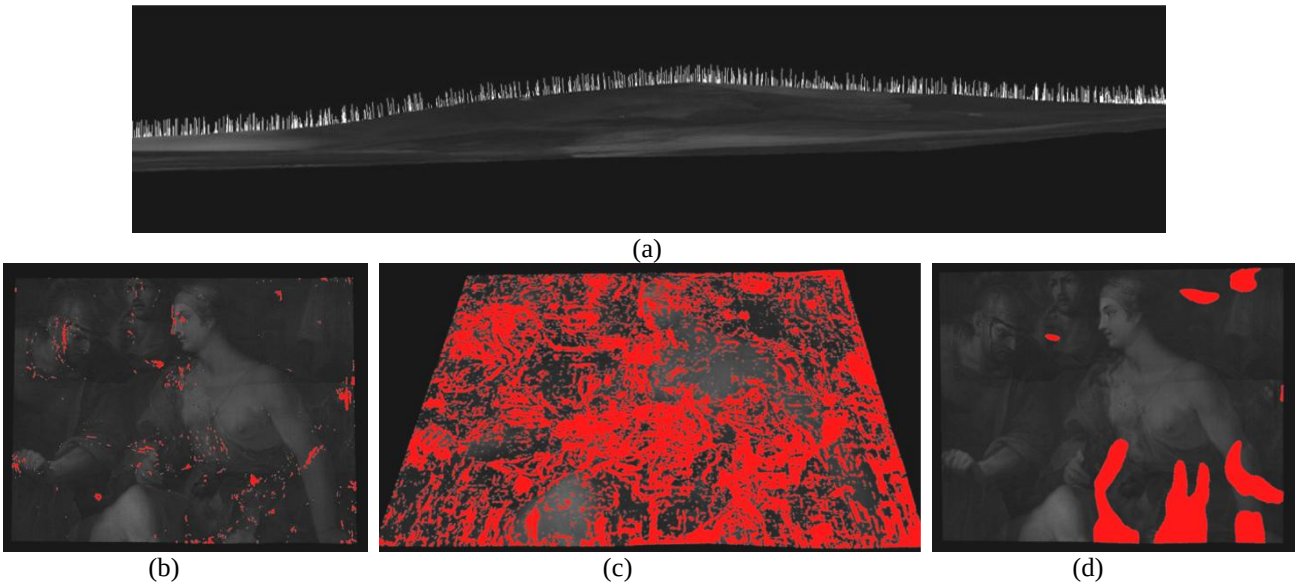

(a)

(b) (c) (d)

Figure 7. Sample of mechanical deterioration, where: (a) Surface normals plotted on the 3D mesh surface; (b) non-flat surface areas on small scale analysis; (c) a 3D display view with detected non-flat surface regions layer in medium scale analysis; (d) a 3D display view with detected non-flat surface regions layer in large scale analysis.

6. CONCLUSIONS

This paper shows the main steps of the processing in the Syddarta project. 3D shape and hyperspectral data are recorded using the prototype hardware. Algorithms for chemical and mechanical analysis of the data are shown. Surface deformations can be identified and localized using the differences of normal vectors approach.

In the near future we will improve some of the steps showed in the previous methodology. In particular, we are dealing with the most appropriate method to fuse hyperspectral bands in order to reconstruct a single image with the projected

pattern. We are also finishing tests to determine the proper classifier for assessing chemical deterioration, where some data regarding to deterioration caused by pollutants needs to be added to the generated database. Finally, we are implementing a model that converts phase-to-height information according to [9], as our actual implementation makes use of empirically-based conversion models.

ACKNOWLEDGEMENTS

This work is part of the ongoing development being currently carried out in SYDDARTA project (www.syddarta.eu), funded by the European Commission under the 7th Framework Programme (project number 265151).

REFERENCES

[1] Hartley, R. and Zisserman, A., "Multiple view geometry in computer vision," Cambridge University Press, 2nd Edition (2003).
[2] Wöhler, C., "3D Computer Vision – Efficient Methods and Applications," Springer (2009).
[3] Sotoodeh, S., "Outlier detection in LASER Scanner Point Clouds," IAPRS Vol. XXXVI, Part 5, Dresden (2006).
[4] Jenke, P. and Wand, M., "Bayesian point cloud reconstruction", Eurographics, Vol. 25 (3), (2006).
[5] Weber, C., Hahmann, S. and Hagen, H., "Sharp feature detection in point clouds," IEEE International Conference on Shape Modeling and Applications (2010).
[6] Kalogerakis, E., Nowrouzezahrai, D., Simari, P. and Singh, K., "Extracting lines of curvature from noisy point clouds," Elsevier Journal of Computer-Aided Design, Special Issue on Point-Based Computational Techniques, 41(4), 282-292 (2009).
[7] Zhang, Z., "A Flexible New Technique for Camera Calibration," IEEE Trans. Pattern Anal. Mach. Intell., 22(11), 1330-1334 (2000).
[8] Brown, D., "Close-range camera calibration," Photogrammetric Engineering, 37(8), 855-866 (1971).
[9] Rajoub, B.A., D.R. Burton, and Lalor, M.J., "A new phase-to-height model for measuring object shape using collimated projections of structured light," Journal of Optics A: Pure and Applied Optics, 7(6), S368 (2005).
[10] Takeda, M., H. Ina, and Kobayashi, S., "Fourier-transform method of fringe-pattern analysis for computer-based topography and interferometry," J. Opt. Soc. Am., 72(1), 156-160 (1982).
[11] Takeda, M. and K. Mutoh, "Fourier transform profilometry for the automatic measurement of 3-D object shapes," Appl. Opt., 22(24), 3977-3982 (1983).
[12] Fujigaki, M. and Morimoto, Y., "Accurate shape measurement for cylindrical object by phase-shifting method using Fourier transform," Proc. SPIE 2921, 557-562 (1997).
[13] Lowe, D.G., "Distinctive Image Features from Scale-Invariant Keypoints," International Journal of Computer Vision, 20(2), 91–110 (2004).
[14] Bay, H., T. Tuytelaars, and Gool, L.V., "SURF: Speeded Up Robust Features," Proc. European Conference on Computer Vision (2006).
[15] Alexa, M., J. Behr, D. Cohen-Or, S. Fleishman, D. Levin, and Silva, C. T., "Point set surfaces," Proc. of the IEEE Conference on Visualization, 21-28 (2001).
[16] Rusu, R.B.,"Semantic 3D Object Maps for Everyday Manipulation in Human Living Environments," PhD Thesis, Technical University of Munich, <http://files.rbrusu.com/publications/RusuPhDThesis.pdf>, (2009).
[17] Castanys, M., M.J. Soneira, and R. Perez-Pueyo, "Automatic Identification of Artistic Pigments by Raman Spectroscopy Using Fuzzy Logic and Principal Component Analysis," Laser Chemistry, 1-8 (2006).